

# Defect-related density of states in low-band gap $\text{In}_x\text{Ga}_{1-x}\text{As}/\text{InAs}_y\text{P}_{1-y}$ double heterostructures grown on InP substrates

T. H. Gfroerer,<sup>a)</sup> L. P. Priestley, and F. E. Weindruch  
*Department of Physics, Davidson College, Davidson, North Carolina 28036*

M. W. Wanlass  
*National Renewable Energy Laboratory, Golden, Colorado 80401*

(Received 19 February 2002; accepted for publication 24 April 2002)

We have measured the excitation-dependent radiative efficiency in a set of lattice-matched  $\text{In}_x\text{Ga}_{1-x}\text{As}/\text{InAs}_y\text{P}_{1-y}$  double heterostructures incrementally lattice mismatched to InP substrates. We find that the overall rate of defect-related recombination shows little change from the lattice-matched case. However, the excitation-dependent transition between defect-related and radiative recombination changes dramatically with mismatch. While a simple defect recombination model assuming defect levels concentrated near the middle of the band gap fits well for the lattice-matched material, the model does not fit the shape of the efficiency curve for the mismatched structures. We show that the addition of band edge exponential tails to the defect-related density of states gives a much better theoretical fit. © 2002 American Institute of Physics.  
 [DOI: 10.1063/1.1487449]

Thermophotovoltaic (TPV) energy conversion systems that utilize broadband, blackbody-like radiators require high-performance, low-band gap (0.4–0.7 eV) photovoltaic converters.<sup>1</sup> Our approach to meeting this requirement involves a converter design based on a lattice-matched (LM)  $\text{InAs}_y\text{P}_{1-y}/\text{In}_x\text{Ga}_{1-x}\text{As}/\text{InAs}_y\text{P}_{1-y}$  double-heterostructure device (LM when  $y=2.14x-1.14$ ), which is grown lattice-mismatched (LMM) on an InP substrate with an intervening compositionally step-graded region of  $\text{InAs}_y\text{P}_{1-y}$ . The low-band gap  $\text{In}_x\text{Ga}_{1-x}\text{As}$  alloy serves as the light absorber and the LM  $\text{InAs}_y\text{P}_{1-y}$  cladding layers passivate the interfaces and confine carriers in the  $\text{In}_x\text{Ga}_{1-x}\text{As}$  material. Deleterious effects of the LMM (e.g., dislocation formation and morphological defects) are alleviated by including an appropriate number of  $-0.2\%$  mismatch  $\text{InAs}_y\text{P}_{1-y}$  steps between the substrate and the double heterostructure.<sup>2</sup>

The lowest band gap ( $\sim 0.5$  eV at room temperature)  $\text{In}_x\text{Ga}_{1-x}\text{As}$  alloys under investigation experience severe (up to  $-1.7\%$ ) LMM, which usually leads to large increases in the rate of defect-related recombination. For TPV applications, such an increase in carrier recombination is problematic because it reduces the conversion efficiency of the cells. Our step-graded design, combined with the passivation afforded by LM  $\text{InAs}_y\text{P}_{1-y}$  cladding layers, has resulted in dramatic improvements in converter performance. In this letter, we explore the physical basis for these improvements by considering the effect of LMM on defect-related recombination in the  $\text{In}_x\text{Ga}_{1-x}\text{As}$  layer. We report excitation-dependent radiative efficiency measurements on several different epitaxial structures that range from the LM condition ( $x=0.53$ ) where no grading is employed to step-graded structures accommodating significant LMM ( $x=0.60, 0.72, \text{ and } 0.78$ ).

We measure the radiative efficiency as a function of excitation power at 77 K to study the changeover between

defect-related (nonradiative) and radiative recombination in the structures (see Fig. 1). The band gap energy in the active layer ( $E_g$ ) is determined from 77 K photoluminescence spectra. Since Auger recombination is slow at low temperatures and defect recombination saturates at high carrier densities, we scale the peak internal quantum efficiency to 100% at 77 K. The low-temperature, high-excitation result provides a

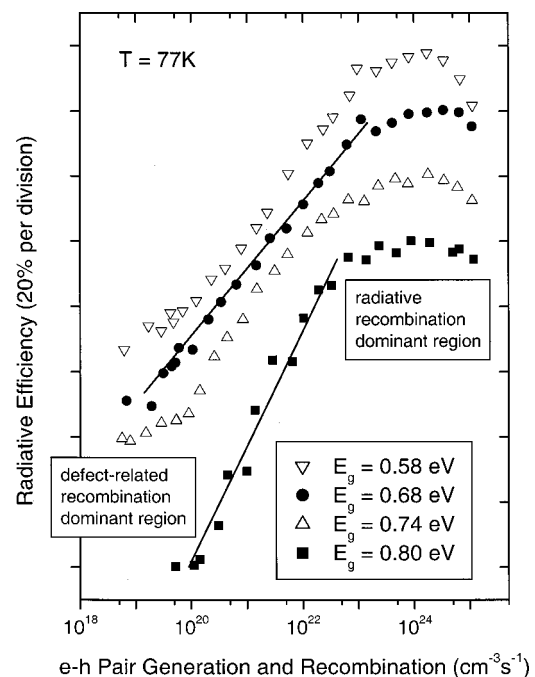


FIG. 1. Internal radiative quantum efficiency (integrated photoluminescence intensity divided by the excitation power) vs the rate of electron-hole pair generation and recombination in steady state. Structures are identified by the InGaAs band gap energy at 77 K. All curves are scaled to 100% peak efficiency and incrementally shifted by 20% for clarity. The solid lines are included to emphasize the difference in the shape of the efficiency curve for the nominally lattice-matched ( $E_g=0.80$  eV) and mismatched structures.

<sup>a)</sup>Electronic mail: tfgfroerer@ davidson.edu

baseline for calibrating measurements at other excitation intensities. In the smallest band gap ( $E_g = 0.58$  eV) alloy, onset of the nonradiative Auger mechanism is evident at the highest excitation rates, even at 77 K. Nevertheless, the plateau in the efficiency curve is wide enough to confirm that the radiative efficiency is nearly 100%. Measurements at higher temperatures, where the efficiency curves do not approach 100%, always have narrower excitation-dependent efficiency peaks.

In Fig. 1, the radiative efficiency grows as the steady-state electron-hole excitation rate approaches the threshold for saturating the defect-related recombination mechanism. While increasing LMM is expected to generate larger defect densities, which typically augment the nonradiative process, we find that this threshold shows little change from the LM case. This observation is consistent with low-injection transient measurements, which show microsecond lifetimes in similar structures.<sup>2</sup> The results are very unusual, but they may be explained by another unique feature of the data shown in Fig. 1: the shape of the efficiency curve changes dramatically between the LM ( $E_g = 0.80$  eV) and LMM ( $E_g = 0.74, 0.68,$  and  $0.58$  eV) structures.

A similar phenomenon has been observed in other systems with treated free surfaces.<sup>3</sup> The effect is attributed to changes in the energetic distribution of surface states in the band gap of the material. When the excitation is intermediate between the defect and radiative recombination dominated regimes, the quasi-Fermi levels for electrons and holes split away from the low-excitation pinned position and move toward their respective band edges. The quasi-Fermi levels determine the energy range of defect states that contribute to recombination. Thus, the photoluminescence (PL) efficiency in this transition region is very sensitive to the energetic distribution of defect states. Variation in the slope of the efficiency curve with increasing excitation is used to map the distribution of defect states within the gap.

The statistics of recombination through defect states depends strongly on the position of the associated energy levels within the band gap.<sup>4</sup> When a carrier is captured at a defect site, the escape probability depends on the proximity of the trap energy to the corresponding band edge. If all of the defect levels are concentrated near the middle of the band gap, the escape probability goes to zero and the defect-related Shockley–Read–Hall (SRH) recombination rate simplifies to a linear dependence on the photoexcited density of electron-hole pairs. Since the radiative rate is proportional to the square of the carrier density, the radiative efficiency is given by

$$\eta = \frac{Bn^2/N}{An + Bn^2/N},$$

where  $n$  is the photoexcited carrier density and  $A$  and  $B$  are coefficients that describe the strength of the SRH and radiative mechanisms, respectively. The photon recycling factor  $N$  accounts for the possibility of PL reabsorption in the active region and connects relative external radiative efficiency measurements with the internal quantum efficiency. As shown in Fig. 2, this simple defect recombination model fits rather well in the LM case.

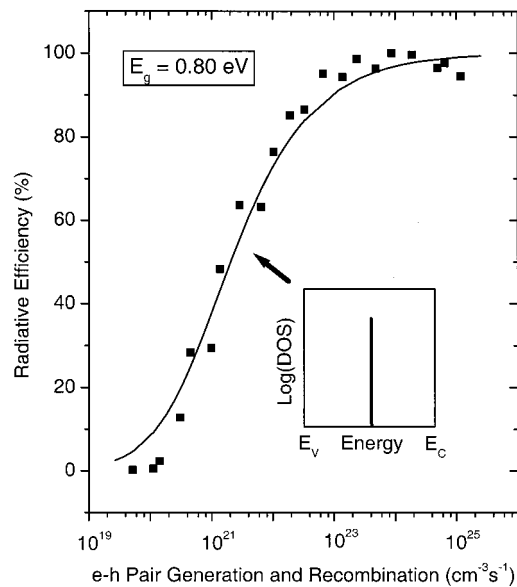


FIG. 2. Internal radiative quantum efficiency vs the steady-state rate of electron-hole pair generation and recombination for the nominally lattice-matched structure. The theoretical fit to the data assumes a discrete DOS for defect levels, which is concentrated near the middle of the band gap as shown ( $E_v$  and  $E_c$  represent the valence and conduction band edges, respectively).

However, as indicated in Fig. 3, the model does not fit the shape of the efficiency curve for the LMM samples. We have developed a computer simulation based on the complete recombination theory that allows for other distributions of energy levels associated with defects. For the LMM structures, we find that addition of band edge exponential tails to the defect-related density of states (DOS) gives a much better theoretical fit (see Fig. 3). A similar distribution was used to fit the results of transport measurements on amorphous silicon<sup>5</sup> and AlGaAs/InGaAs/GaAs heterostructures.<sup>6</sup> The tail states can be attributed to local distortions of the bonding configuration in the interface region.<sup>7</sup>

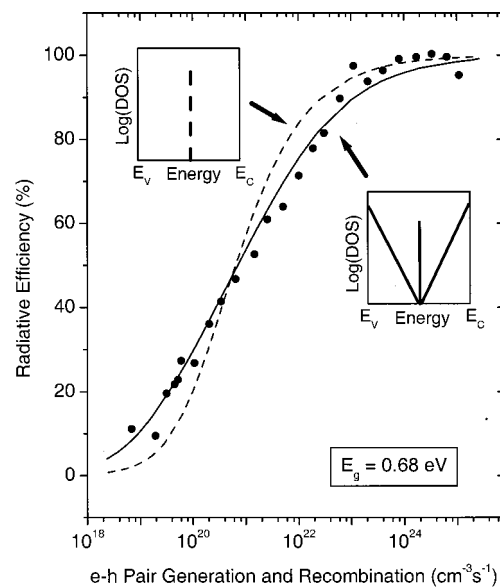


FIG. 3. Internal radiative quantum efficiency vs the steady-state rate of electron-hole pair generation and recombination for a moderately mismatched structure. The theoretical fits correspond to the defect-level DOS functions indicated in the inset graphs.

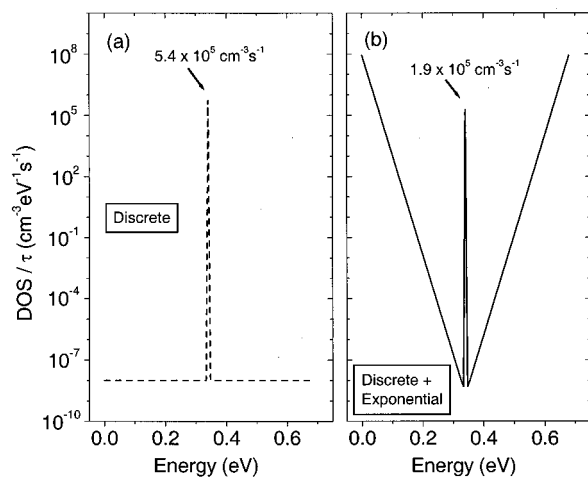


FIG. 4. Defect-related DOS functions (divided by the capture time  $\tau$ ) used to obtain the theoretical fits shown in Fig. 3. Energy is measured from the valence band edge.

Details of the DOS functions used in the theoretical fits are shown in Fig. 4. The capture time  $\tau$  is defined as the reciprocal of the probability per unit time that a carrier will be captured for the case in which the traps are all empty. Hence,  $\tau$  is a measure of the fraction of space swept out by a moving carrier in a given period of time. One very surprising feature of Fig. 4(b) is the reduction of defect states concentrated near the center of the gap relative to the discrete fit. This result suggests that LMM does not simply add states near the band edges, but also moves some levels from the center to the edges of the gap.

We should note that our modeling procedure does not generate a unique solution for the density of states function. The concentration of defect states at the band edges and the characteristic energy of the exponential tails can be modified somewhat and still yield reasonable fits. However, the model is capable of identifying important qualitative features in the underlying distribution of defect levels. For example, flat distributions with a constant DOS across the gap produce efficiency curves that closely resemble those for the discrete

distribution. Hence, a flat distribution is also inconsistent with our LMM results. We can generally conclude that the LMM structures have a relatively high concentration of defect levels near the band edges. Deep level transient spectroscopy experiments are underway to verify the DOS profiles indicated here.

In conclusion, radiative efficiency measurements show surprisingly low SRH recombination rates in our LMM structures and the physics underlying this special behavior has remained largely a mystery. However, the results reported in this letter contain a unique feature that may explain the superior performance of this system: the shape of the efficiency curve changes dramatically between the LM and LMM cases. Good theoretical fits are only obtained when the distribution of defect states in the LMM structures is assumed to be fundamentally different from that of the LM system. We find that defect states are concentrated near the band edges where they are less likely to facilitate nonradiative recombination. This discovery represents an important step in understanding what distinguishes these states from the nonradiative centers that are typically found in LMM epistuctures.

The authors would like to thank J. J. Carapella for performing the metalorganic vapor phase epitaxy growth. This research was supported by Research Corporation. Acknowledgement is also made to the donors of The Petroleum Research Fund, administered by the ACS, for partial support of this work.

<sup>1</sup>M. W. Wanlass, J. S. Ward, K. A. Emery, M. M. Al-Jassim, K. M. Jones, and T. J. Coutts, *Sol. Energy Mater. Sol. Cells* **41/42**, 405 (1996).

<sup>2</sup>R. K. Ahrenkiel, S. W. Johnston, J. D. Webb, L. M. Gedvilas, J. J. Carapella, and M. W. Wanlass, *Appl. Phys. Lett.* **78**, 1092 (2001).

<sup>3</sup>T. Saitoh, H. Iwadate, and H. Hasegawa, *Jpn. J. Appl. Phys., Part 1* **30**, 3750 (1991).

<sup>4</sup>W. Shockley and W. T. Read, Jr., *Phys. Rev.* **87**, 835 (1952); R. N. Hall, *ibid.* **87**, 387 (1952).

<sup>5</sup>F. Wang and R. Schwarz, *Phys. Rev. B* **52**, 14586 (1995).

<sup>6</sup>H. Tomozawa, K. Numata, and H. Hasegawa, *Appl. Surf. Sci.* **60/61**, 721 (1992).

<sup>7</sup>H. Hasegawa, L. He, H. Ohno, T. Sawada, T. Haga, Y. Abe, and H. Takahashi, *J. Vac. Sci. Technol. B* **5**, 1097 (1987).